CASE WESTERN RESERVE UNIVERSITY

Discussions

Volume 2 | Issue 1 Article 7

2023

# Effects of Neural Lesions on a Context-Dependent Molluscan Muscle

Amanda Hong
*Case Western Reserve University*



## Recommended Citation

Hong, Amanda (2023) "Effects of Neural Lesions on a Context-Dependent Molluscan Muscle," *Discussions*: Vol. 2: Iss. 1, Article 7.
DOI: https://doi.org/10.28953/2997-2582.1080
Available at: https://commons.case.edu/discussions/vol2/iss1/7

# Effects of Neural Lesions on a Context -Dependent Molluscan Muscle

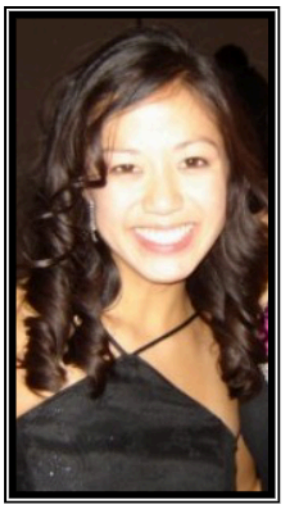


## -Amanda Hong-

Amanda Hong is a third-year student double-majoring in biochemistry and economics with a pre-med emphasis. Beyond her research involvement in the Biology department, Amanda is actively involved on campus. She has held leadership positions within the Journal Distribution Project, the Panhellenic Council, and her sorority Alpha Phi. In addition, she currently serves on the chapter executive boards of both the Golden Key International Honour Society and the Mortar Board Honor Society. Furthermore, she is an active member of the Student Turning Point Society, Order of Omega Honor Society, and Gamma Sigma Alpha Honor Society, as well as a volunteer at Rainbow Babies Children's Hospital.



### *-Acknowledgements-*

I would like to thank my research mentor, Dr. Hillel Chiel, for all of his time and effort throughout the past year. He has truly been a supportive and inspirational guide during the summer research program period and well into the academic year. Furthermore, I would like to thank Jeff McManus, my graduate student mentor. This project would not have been possible without his constant guidance and support. Jeff was instrumental in the execution and completion of this research project. Finally, I would like to thank Joseph (JT) Tan, another graduate student, for his assistance in demonstrating essential laboratory procedures.



## ABSTRACT

Many muscles may have more than one function depending on their mechanical context. For example, in the human arm, the brachioradialis contributes to pronation when the hand is supinated, and to supination when the hand is pronated. We are interested in studying muscles whose function is context dependent, that is, the direction of the force or torque that they generate changes sign as a function of their mechanical context. Previous modeling studies have suggested that the posterior part of the I1/I3/jaw complex in the mollusk *Aplysia californica* can change the direction of the forces it exerts as a function of its mechanical context. In particular, when the grasper (radula/odontophore) is behind the I1/I3/jaw complex, the muscle acts to push the grasper towards the esophagus, i.e., to retract it. A kinetic model and *in vivo* studies of the I1/I3/jaw complex using magnetic resonance imaging suggest that when the grasper is anterior to the back part (posterior) of the I1/I3/jaw complex, which occurs during the strong protractions of biting, the posterior part of the muscle can act to protract the grasper.

To test this hypothesis, we performed unilateral lesions on individual branches of the nerve that innervates the I1/I3/jaw complex, buccal nerve 2 (BN2). Its three branches (referred to as "a", "b", and "c") have been shown to have different effects on the I1/I3/jaw complex. Specifically, shocking branches "a" and "c" causes the anterior part of the I1/I3/jaw complex to contract, whereas shocking branch "b" causes the posterior part of the I1/I3/jaw complex to contract. We therefore hypothesized that uni-

lateral lesions of branch "b" (BN2-b) would cause deficits of the peak protraction of biting. Results show that unilateral lesions of the other two branches of BN2 cause no significant changes in biting behavior, whereas unilateral lesions of BN2-b cause a specific deficit in biting. At the peak of normal biting protractions, the radula remains protracted for an extended period of time. After the BN2-b unilateral lesion, the radula begins to retract significantly faster on the side ipsilateral to the lesion. These results support the hypothesis because they suggest that forces that would ordinarily be expressed in the posterior part of the I1/I3/jaw complex are necessary for the radula to remain protracted for an extended period of time near the peak of biting. These studies will help to clarify the neural control of context dependent muscles in many other animals.

## INTRODUCTION

In order to understand the relationship between neural signals and their corresponding movements and behavioral responses, the muscular function involved must also be understood. However, the role of muscular function may be complicated, because a muscle may exhibit more than one function depending on its mechanical context. A previous study using cadaver specimens and computer modeling showed that the moment arms of muscles crossing the elbow are substantially dependent upon forearm and elbow position. In particular, these experimental results showed that elbow flexion moment arms increase substantially with elbow flexion and are greatly affected by the pronation/supination angle (Murray *et al.* 1995). In other words, the brachioradialis muscle in the human arm contributes to moving the forearm in opposite directions, depending on the initial position of the arm. Another study quantified the effects of postural variation in the biomechanics of six human shoulder muscles. Results showed that the mechanical function of each muscle varied substantially with arm posture. This variation was dependent upon one or more angles defining arm posture within the respective frame of reference (Buneo *et al.* 1997). Another study used similar methods to characterize the mechanical actions of the hindlimb muscles of the cat. Results showed that the cat flexor and extensor muscles generated large extra-sagittal torques that were joint angle dependent with regards to both magnitude and sign (Lawrence and Nichols, 1999a, Lawrence and Nichols, 1999b).

These studies suggest that the mechanical function of a muscle may be context-dependent in that the direction of the force or torque they generate changes sign as a function of their mechanical context. Previous research has explored the functional relationships between neural control and muscular behavior through methods such as biomechanical modeling. However, in many species, the complexity of the organism's nervous system makes in depth studies impractical. The marine mollusk *Aplysia Californica* is an ideal organism for experimental study due to its relatively simple nervous system. Commonly known as the sea slug, *Aplysia* has large identifiable neurons and an easily accessible buccal mass, or feeding apparatus. Feeding behaviors are also easily elicited by tactile stimulation with seaweed laver, facilitating observation of biting behaviors.

*Aplysia* feeding structures lack a hard skeletal system, and instead function through forces provided by muscle and cartilage. Due to the many degrees of freedom and great flexibility in movement, comprehension

of biomechanical properties is necessary in understanding the neural control. Previous kinematic and kinetic modeling studies have suggested that the posterior part of the I1/I3/jaw complex in *Aplysia californica* can act in a context dependent manner through its ability to change the direction of the forces it exerts as a function of its mechanical context.

The jaw musculature's context-dependent function was previously tested through a kinetic model of the buccal mass. This model tested the mechanical advantage as the radula/odontophore moved during biting behaviors (Sutton *et al.* 2004). They found that early activation of the I1/I3 muscle complex could indeed assist in moving the radula/odontophore in the anterior direction during protraction.

Magnetic resonance imaging data further supports the context-dependent hypothesis through imaging of the internal structures of the buccal mass. The temporal and spatial resolution of the experimental images enabled direct measurement of the anteroposterior lengths of the I1/I3/jaw musculature both dorsally and ventrally, and thus facilitated kinematic measurements of the muscles of the buccal mass during swallowing behaviors (Neustadter *et al*. 2002b). These studies showed that the radula/odontophore midline is anterior to only the posterior half of I1/I3 during peak protraction in biting. Therefore, only this posterior half would be capable of intensifying protraction, advocating that this posterior I1/I3 acts in a context-dependent manner.

In fact, the I1/I3 muscle complex may have context-dependent effects that intensify protraction during biting and retraction during swallowing, as shown by magnetic resonance images and I1/I3 lesions. Observations of the buccal mass have shown that the hinge muscle also aids in moving the anterior portion of the radula/odontophore into position to allow the I1/I3/jaw complex to push the radula/odontophore strongly in the posterior direction (Ye *et al.* 2006). The kinetic model shows that the function of the I1/I3 muscle can be changed by modifying the timing of I2 and I1/I3 muscle activations in relation to each other. The model showed that if activation of I3 begins during the protraction phase while I2 is still being activated and the radula/odontophore has not yet returned to rest, the radula/odontophore will then protract more strongly and for a longer period of time. This behavior was tested through implantation of extracellular electrodes in the I2 muscle and on buccal nerve 2 (Chiel *et al.*, unpublished observations).

Kinematic models suggest that the I3 muscle plays an important role in retraction during swallowing, and further suggest that if I3 is anterior to the midline of the radula/odontophore when at rest, contraction of I3 will induce movement in the posterior direction, and vice versa (Neustadter *et al.* 2002a). Previous lesion studies testing this context-dependent hypothesis included I3 cartilage lesions and bilateral BN2 lesions, comparing jaw widths, rates of ingestion and rejection, and time from peak protraction to jaw closure. The I3 cartilage lesions prevent the I1/I3 muscle complex from fully closing the lumen of the jaws without affecting the neural innervation. BN2 lesions, on the other hand, remove the neural innervation of the I1/I3 muscles, effectively paralyzing the I1/I3 muscles with the exception of passive forces. The effects of these lesions reduced the intensity of both the protraction and retraction phases during biting and rejection, respectively (Chiel *et al.*, unpublished observations).

Other lesion studies explored the effects of bilateral lesions of each of the branches of buccal nerve 2. It was known that buccal nerve 2 innervates the I1/I3 muscle complex; however, the effects of a single-branch lesion on I1/I3 and radula/odontophore behavior were unknown. This study showed that a lesion on buccal nerve 2 branch b resulted in a reduction in biting protraction for animals performing large amplitude bites (McManus, unpublished observations).

This experiment focuses on the effects of a unilateral lesion on buccal nerve branch b, and thus tests the hypothesis that the posterior I1/I3 exerts a protractive force during biting.

Figure 1. Schematic view of camera set-up apparatus and camera angles.

## MATERIALS AND METHODS

*Observations and Lesion studies*

*Aplysia Californica* (Marinus, Long Beach, California) marine mollusks ranging from 200 to 500 grams in weight were randomly chosen after being aroused to food, and demonstrating vigorous biting responses. In order to obtain behavior identical to that in natural conditions, observations were performed in fresh artificial seawater produced from Instant Ocean sea salt mix. The tanks were maintained at temperatures between 14 to 17 degrees Celsius and at a salinity level of approximately 36ppt. Bio-Bag disposable filter cartridges were used to ensure that the environment of the mollusks was kept in acceptable condition.

The *Aplysia* specimen was then placed in a large Petri dish after obtaining its weight by difference. Prelesion behavior was observed through video recording using two Canon NTSC 2R60 digital video camcorders in a two-axis configuration with an algorithm for three-dimensional reconstruction video analysis (algorithm designed by Gregory Sutton and Jeff McManus; camera

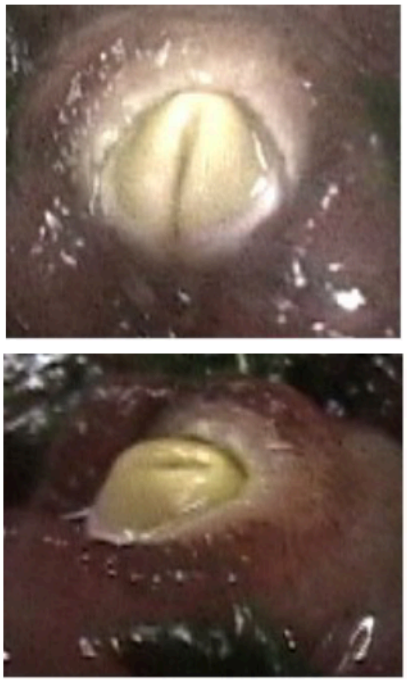

Figure 2. Views from each camera. The picture on the left shows the view from camera 1, and the picture on the right shows the view from camera 2.

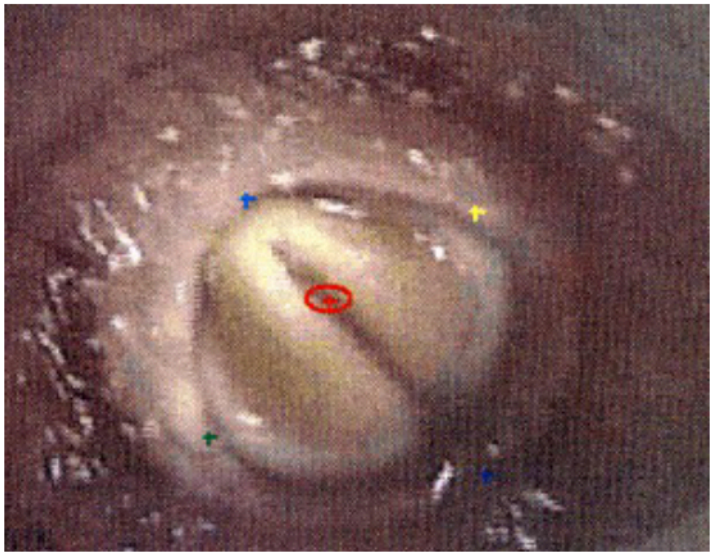

Figure 3. Frame showing the five points plotted on the jaw line and radula. A point was placed at both extremities of the jaw (blue points), as well as on both sides approximately in the middle (green and yellow points). A fifth point (red) was placed in the middle

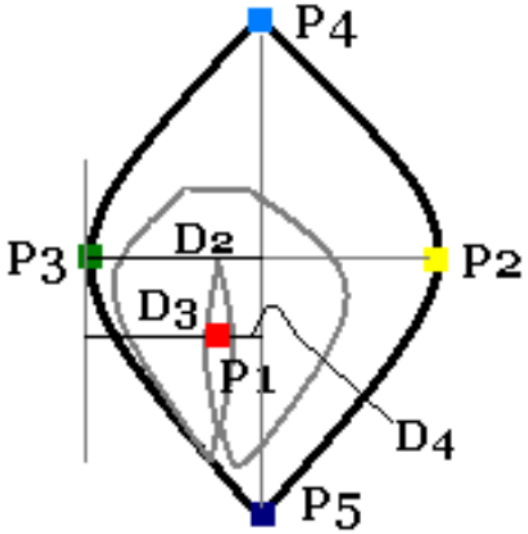


Figure 4. Drawing of radula and jaw with point and distance configurations. D2 and D3 were calculated for both sides of the jaws.

set-up designed by McManus) as shown in Figure 1. The views from each camera are shown in Figure 2.

Biting responses were induced through bilateral stimulus with seaweed laver. This method resulted in a better view of the slug's jaw and protracting radula. After obtaining sufficient footage of biting behavior, the sea slug was placed in a dissecting tray with a small amount of artificial seawater. A perimeter of Styrofoam blocks was then secured around the sea slug with dissecting pins to minimize movement. The edges of the tray beyond the Styrofoam perimeter were then packed with the ice, and the tray was placed in the freezer for approximately fifteen minutes. The Styrofoam blocks were then removed and ice was placed directly on and around the slug. The tray was returned to the freezer for approximately thirty to forty minutes until the slug appeared to be completely relaxed (i.e., anesthetized).

The slug was then pinned to the tray with dissecting pins through its tail and each anterior tentacle. A small incision approximately one centimeter in length was made along the vertical axis of the dorsal side of the specimen, starting approximately one centimeter forward from the rhinophores. This incision was then held open using four paperclips on strings tightly fastened to the edges of the dissecting tray. The buccal mass was rotated to either the left or right side, and a unilateral lesion *in vivo* of buccal nerve 2, branch "b" was performed. After returning the buccal mass to its original orientation, the incision was sutured with Ethicon K-890H 5-0 black braided silk, using a 13 mm Ethalloy™ needle.

The same procedure was followed for control experiments, except that a unilateral lesion *in vivo* of buccal nerve 2, branch "a" or "c" was performed instead. A

total of three experimental and three control trials were completed, consisting of two lesions of the right buccal nerve 2-b, one lesion of the left buccal nerve 2-b, one lesion of the right buccal nerve 2-a, one lesion of the right buccal nerve 2-c, and one lesion of the left buccal nerve 2-c.

After the slug recovered from the lesion surgery (typically about two days after the surgery), and resumed normal eating behavior, post-surgery feeding responses were recorded again with digital camcorders in the two-axis configuration described above.

Once post-surgery behavior was recorded, the lesion was then checked to ensure that nerve re-growth had not occurred. The slug was anaesthetized with injections of 50% isotonic $MgCl_2$ (333 mM) solution until the slug no longer retracted from external stimulation. The buccal mass was then dissected out of the slug and examined under a microscope to ensure the lesion of the nerve branch had no regeneration. For all data reported in this paper, no regeneration was observed.

*Data Analysis*

The video footage was exported to iMovie, and several clips of individual bites were extracted from each pre- and post-surgery trial. Three clips from each trial were analyzed with the WinAnalyze program. Five points were plotted on each frame, starting when the radula halves touched together after peak protraction until the radula had retracted back into the mouth and was no longer clearly discernable. The five points were chosen in order to calculate several distances of interest using the three-dimensional reconstruction coordinates of WinAnalyze. The point configuration is shown in Figure 3.

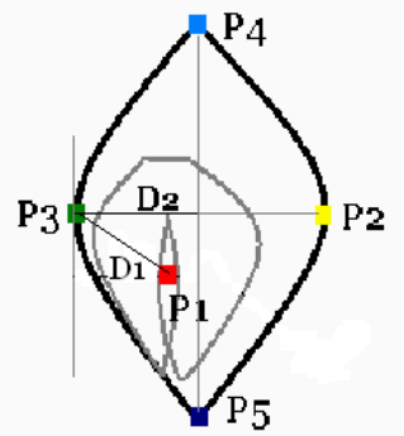


Figure 5. Drawing of radula and jaw with point and distance configuration. D1 and D2 are computed in three-dimensional space without any projection corrections for both sides of the jaw.

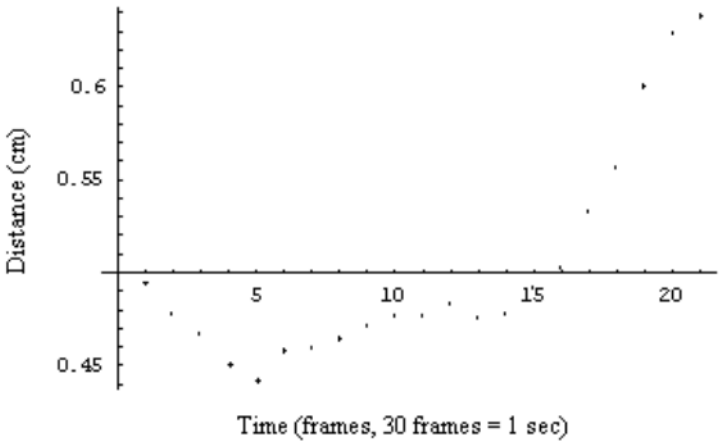


Figure 6. Real distance data from one trial of pre-lesion behavior.

The WinAnalyze three-dimensional reconstruction data was then exported and analyzed using *Mathematica* (analysis program written by Jeff McManus). Evaluation produced graphs showing the projected distance from the bisecting midline to the side of the jaw (D2), the projected distance from the radula center to a line parallel to the side of the jaw (D3), and the projected distance from the radula center to the midline (D4), or radular shift. Figure 4 shows a schematic drawing of the placement of points and the distances of interest.

As shown, P1 is a point in the middle of the radula surface (between the radula halves), P2 and P3 are on the jawline along the sides of the mouth, and P4 and P5 are on the jawline at the front and back corners of the mouth. This is a three-dimensional object resulting in a configuration of non-planar points.

Initial calculations computed the distance in three-dimensional space from the middle of the radula halves to each side of the mouth (D1), and the distance from the bisecting line across the middle of the mouth to either side (D2) as shown by Equations 1 and 2 (point-line distance formula; see Figure 5).

$$D1 = |P3 - P1| \quad (1)$$

$$D2 = |(P5 - P4) \times (P4 - P3)| / |P5 - P4| \quad (2)$$

This configuration was meant to show the faster shift of the radula and jaw closure on the lesioned side as compared to the non-lesioned side. However these distances contain many sources of confounding error due to movement up and down the z-axis (into and out of the mouth). Since the jaw and radula complex is not on a single plane, movement of the radula center (P1) up and down through the jaws can increase both distances, leading to distorted trends. Figure 6 shows a sample of this data.

This is corrected by using a cross product of two existing vectors to form a vector perpendicular to the jaw plane. The two initial vectors are constructed from P4 to P5 (V1) and from P2 to P3 (V2). The resulting vector, V3, can be used to define a plane using any other point. Equation 3 and Figure 7 illustrate these calculations.

$$V3 = V1 \times V2 \quad (3)$$

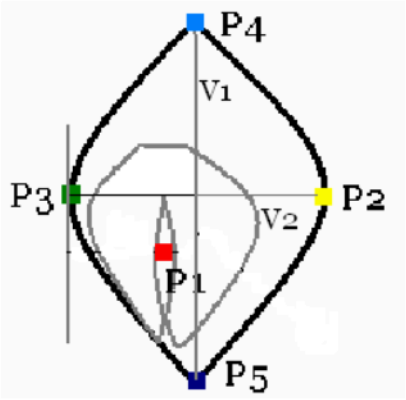


Figure 7. Drawing of radula and jaw showing vector configuration. V3 is the cross product perpendicular to the jaw plane (out of the page).

V3 is then used to find another perpendicular vector from P1 at the split of the radula halves by defining another point, P6, shown in Equation 4. Equation 5 then describes the intersection of the line through P1 and P6 with a plane perpendicular to V3 and containing P2 and P3 (the "jaw plane").

$$P6 = P1 + V3 \quad (4)$$

$$u = V3 \bullet (P3 - P1) / V3 \bullet (P6 - P1) \quad (5)$$

The intersection point, P7, between the line from P1 to

P6 and the jaw plane is then found.

$$P7 = P1 + u(P6 - P1) \quad (6)$$

The resulting distance from P3 to P7 is the projected distance of D1 (as shown in Figure 6). A sample of this data is shown in Figure 8.

Although this counteracts error due to z-axis movement, this projection does not account for error due to forward/backward movement of the radula. To counteract this new source of error, the direct distance from the radula center to a line along the side of the jaw, as shown by D3 in Figure 4, was calculated. This distance was found by defining another point, P8, to form a line parallel to V1 through P3.

$$P8 = P3 + V1 \quad (7)$$

Using the point-line distance formula, the distance from P7 to this new line was calculated, resulting in a projected distance D3 (shown schematically in Figure 4).

$$D3 = |(P8 - P3) \times (P3 - P7)| / |P8 - P3| \quad (8)$$

This projected distance shows the best approximation of the distance from the center of the radula to the side of the mouth. A sample of this data is shown in Figure 9.

This same method of calculation was used to obtain the projected distance from the midline to either side of the mouth, represented as D2 in Figure 4. These projection calculations are necessary to account for error due to z-axis and forward/backward movements of the radula that would otherwise confound and distort changes in distance.

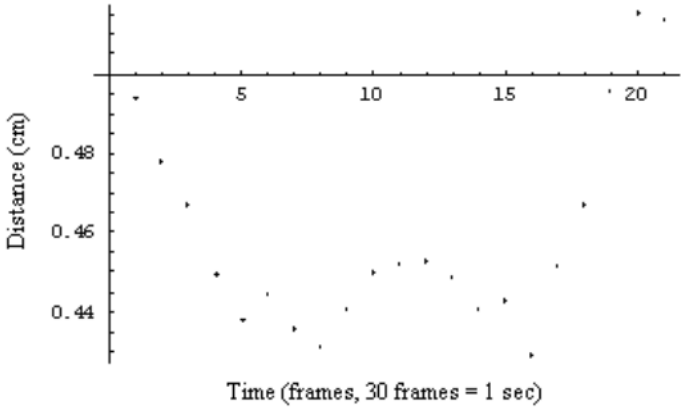


Figure 8. Projected distance D1 from one trial of pre-lesion behavior (same trial as shown in Figure 7).

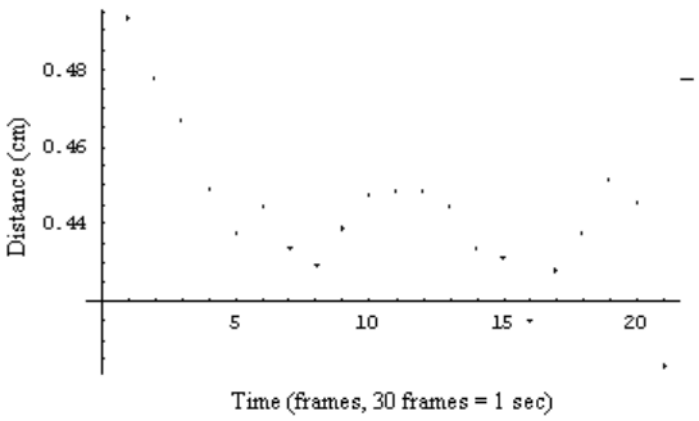


Figure 9. Projected distance data corrected for y-axis movement from one trial of pre-lesion behavior (same trial as shown in Figures 6 and 8).

The last distance of interest is the projected distance from the radula center to the bisecting midline of the jaw, represented as D4 in Figure 4 (reproduced below). This distance is calculated as the difference between the projected distances D2 and D3.

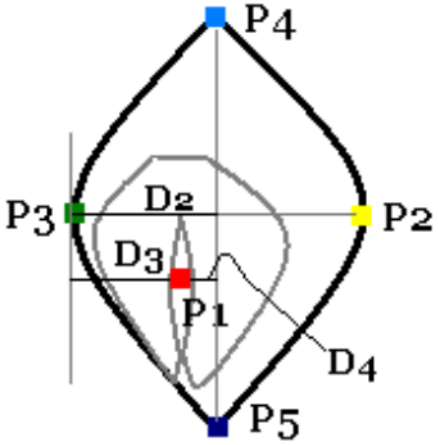


Figure 4. (Reproduced from above) Drawing of jaw and radula with distance and point configurations.

## RESULTS

Qualitative results showed that the length of protraction was reduced in the side with a BN2 branch "b" lesion as a result of a reduced force in that side.

Figures 10 – 13 show results from post-lesion behavior of one animal that underwent a unilateral BN2-b lesion. Time zero is approximately when the radula halves close together immediately after peak protraction. The y-axis measures distance in centimeters and the x-axis measures distance in frames (30 frames = 1 second). The length of observation lasted until the points were no longer discernable for plotting in WinAnalyze.

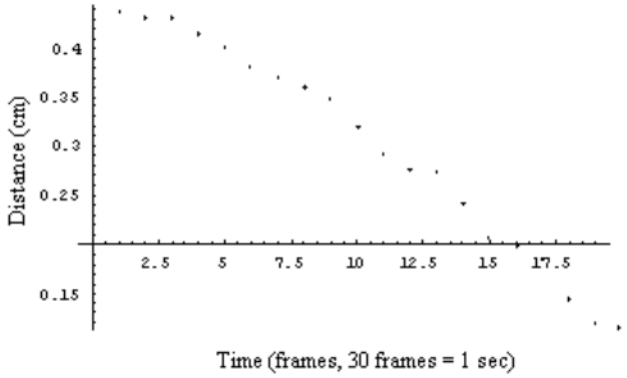


Figure 10. Projected distance (cm) from bisecting midline to jawline along side of mouth as a function of time (frames) for lesioned side. This distance is analogous to D2 defined above.

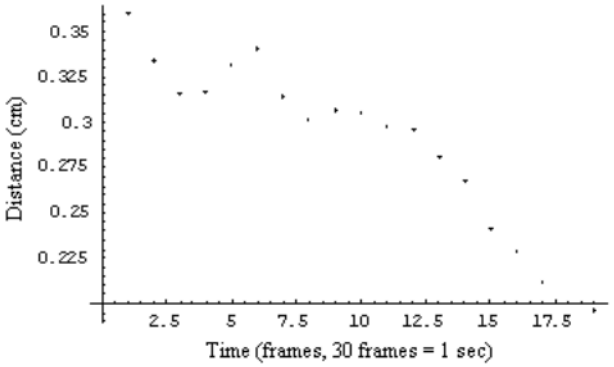


Figure 11. Projected distance (cm) from bisecting midline to jawline along side of mouth as a function of time (frames) for unlesioned side. This distance is analogous to D2 defined above.

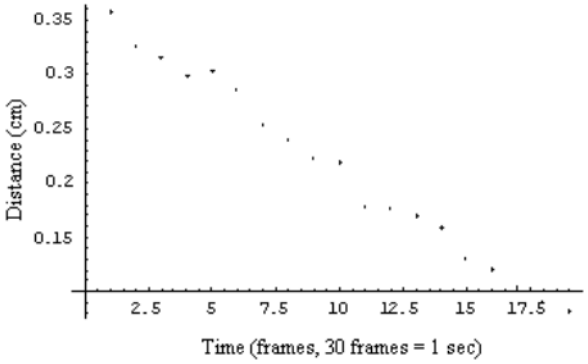


Figure 12. Projected distance (cm) from center of radula to line along side of mouth as a function of time (frames) for lesioned side. This distance is analogous to D3 defined above.

As demonstrated by the graphs above, the lesioned side has a greater rate of change and a greater real change in distance as compared to the unlesioned side. However, comparisons of jaw closure (D2) and radula shift (D3) are difficult to directly compare since changes in these distances may affect each other. Thus, the distances from the radula center to the bisecting midline (D4), or the differences between D2 and D3, were used for analysis and comparison. Figure 14 shows data for the change of D4 over time in the same animal as Figures 10 – 13.

D4 data was compiled for three separate bites from each test animal for both pre- and post-lesion behavior. The distances were then averaged and graphed with standard deviation error bars.

For specimens with a unilateral buccal nerve 2 branch "b" lesion, the pre- and post-surgery behaviors show a significant difference in the amount of radula shift from the bisecting jaw plane midline. As shown in Figure 15, the before surgery average rate of change (slope) was 0.0002 cm/frame, or 0.06 mm/sec. Conversely, the after surgery average rate of change was -1.89 mm/sec (over 30 times greater than the pre-lesion rate of change). For specimens with a unilateral buccal nerve 2 branch "a" lesion, the pre- and post-surgery behaviors did not show any significant difference in the amount of radula shift from the bisecting jaw plane midline. As shown in Figure 16, the before surgery average rate of change was -1.32 mm/sec. Conversely, the after surgery average rate of change was -0.57 mm/sec. The pre-lesion rate of change is not significantly different than the post-lesion rate of change.

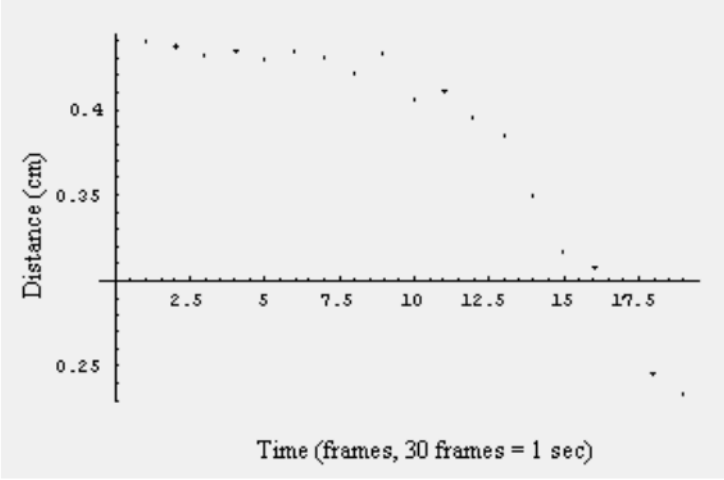


Figure 13. Projected distance (cm) from center of radula to line along side of mouth as a function of time (frames) for unlesioned side. This distance is analogous to D3 defined above.

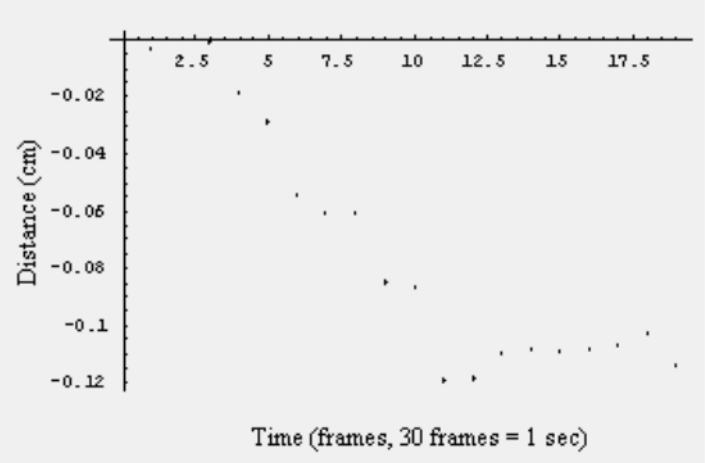


Figure 14. Projected distance (cm) from center of radula to bisecting midline as a function of time (frames) for unilaterally BN2-b lesioned animal. This distance is analogous to D4 defined above.

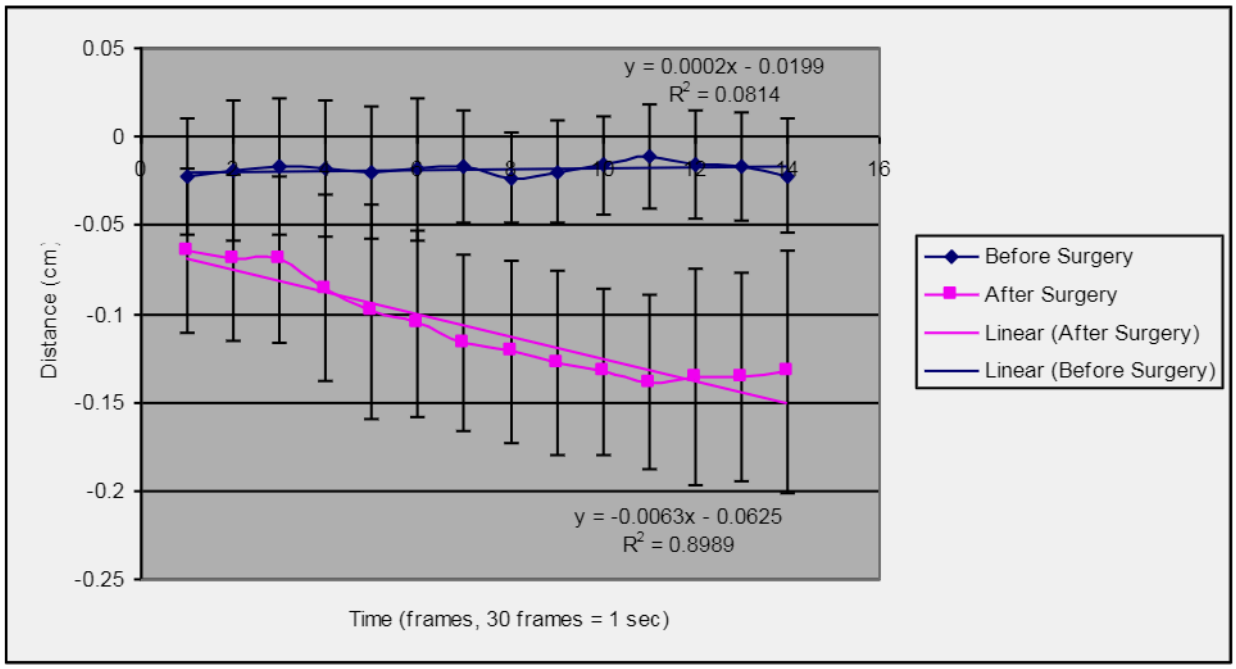


Figure 15. Radula shift distance from the jaw plane midline (D4) during protraction for unilateral buccal nerve 2 branch "b" lesions. This graph is a compilation of data from two sea slugs (N=2), each with three trials for both pre- and post-surgery behavior.

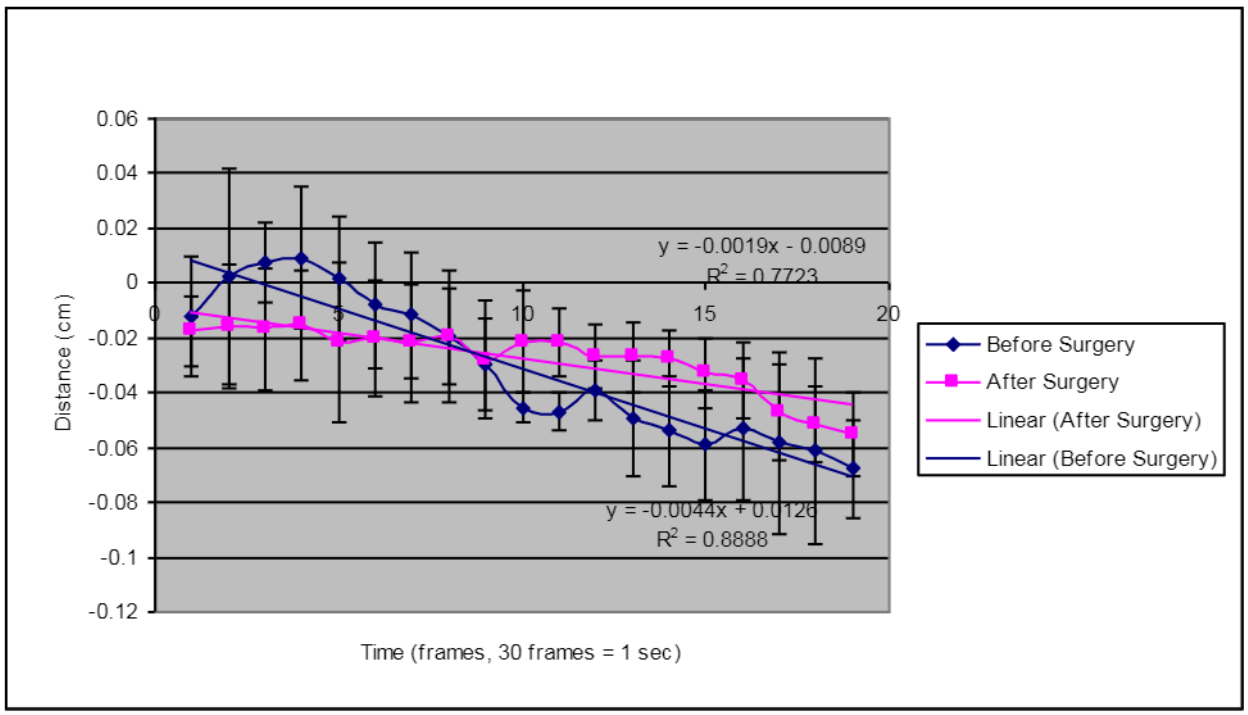


Figure 16. Radula shift distance from the jaw plane midline (D4) during protraction for unilateral buccal nerve 2 branch "a" lesions. This graph is a compilation of data from one sea slug (N=1), with three trials for both pre- and post-surgery behavior.

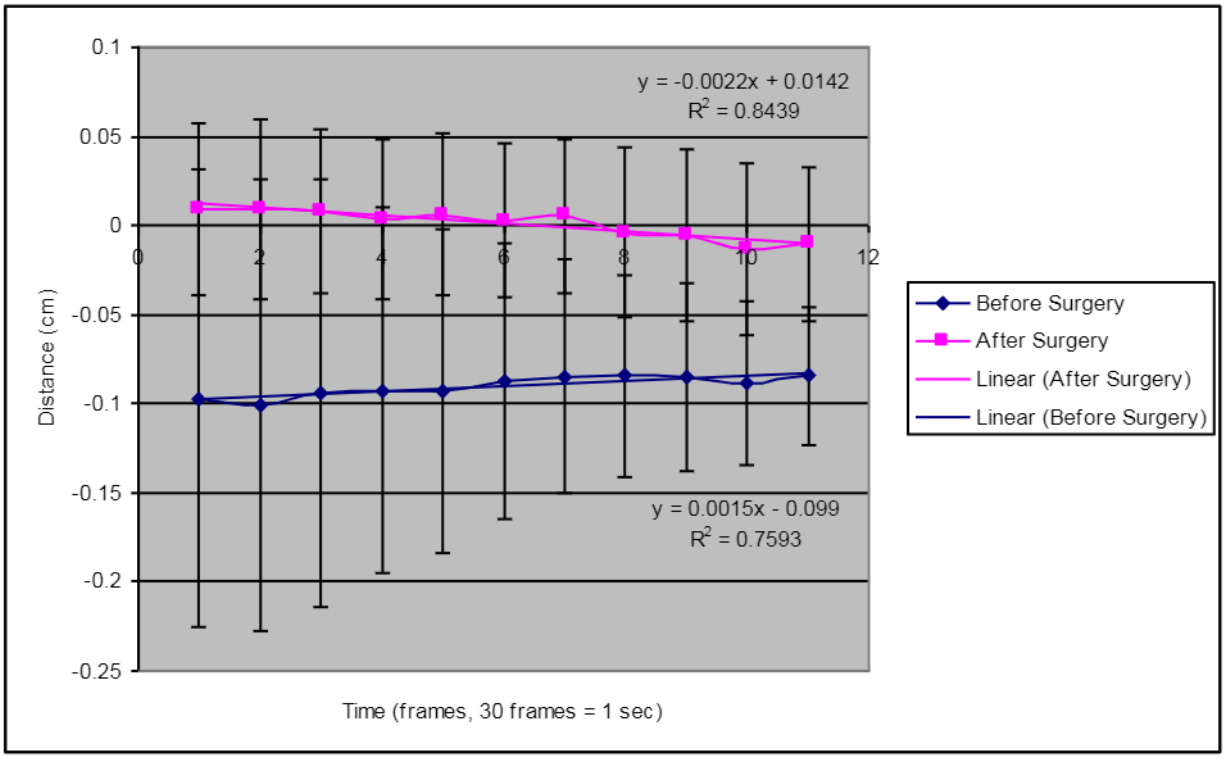


Figure 17. Radula shift distance from the jaw plane midline (D4) during protraction for unilateral buccal nerve 2 branch "c" lesions. This graph is a compilation of data from two sea slugs (N=2), each with three trials for both pre- and post-surgery behavior.

For specimens with a unilateral buccal nerve 2 branch "c" lesion, the pre- and post-surgery behaviors also did not show any significant difference in the amount of radula shift from the bisecting jaw plane midline. As shown in Figure 17, the before surgery average rate of change was 0.45 mm/sec. Conversely, the after surgery average rate of change was -0.66 mm/sec.

Though the initial slope comparison between compiled pre- and post-lesion behavior show significant differences only with a unilateral lesion on BN2-b, there still may be some error in defining significance due to multiple, or unplanned, comparisons. These multiple comparisons include tests of comparisons between all possible pairs of means and introduce error due to possible use of outlying points in the population. To correct for this, we employ statistical comparison of multiple regression lines by first computing the difference between pre- and post-lesion behavior for each test specimen. By calculating the difference in each individual animal as opposed to averaging all data for one particular lesion type, the animal itself is used as its own control. Figure 18 shows an example of this calculation for a single animal.

Furthermore, the observation length is also normalized respective to each individual bite. Normal observation durations vary substantially depending on the number of frames in which the points on the radula and jaw are clearly discernable. Instead of using the least number of frames available for each lesion type, each individual bite observation is normalized by using data

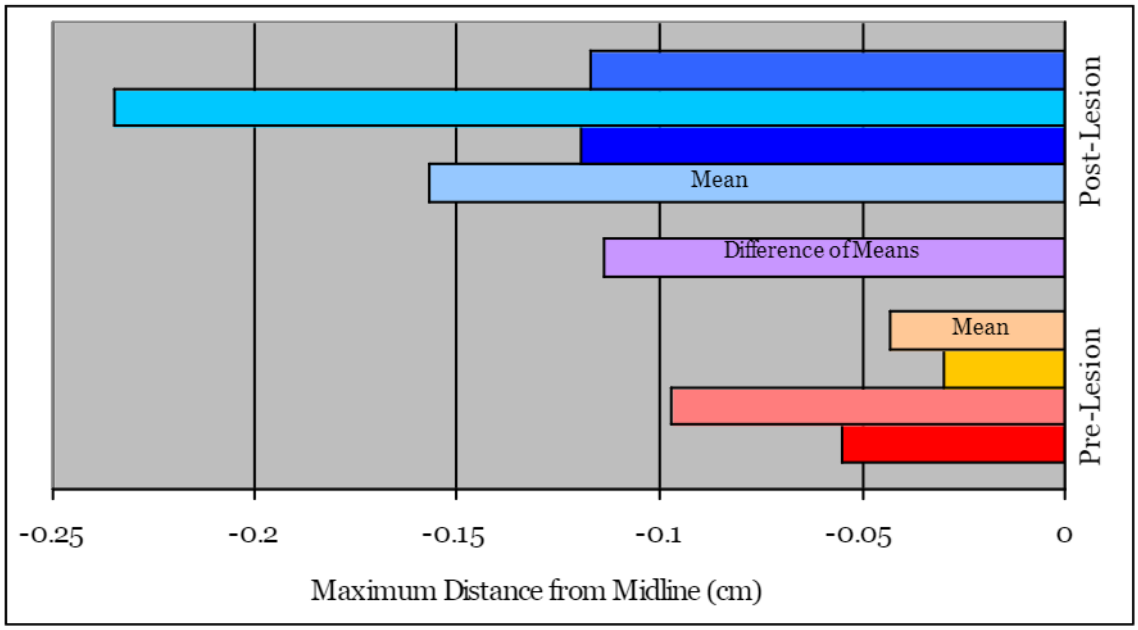


Figure 18. Maximum deviation distance from midline is shown for three bites for both pre-lesion and post-lesion behavior. The difference between the means was calculated as the comparable variable of interest.

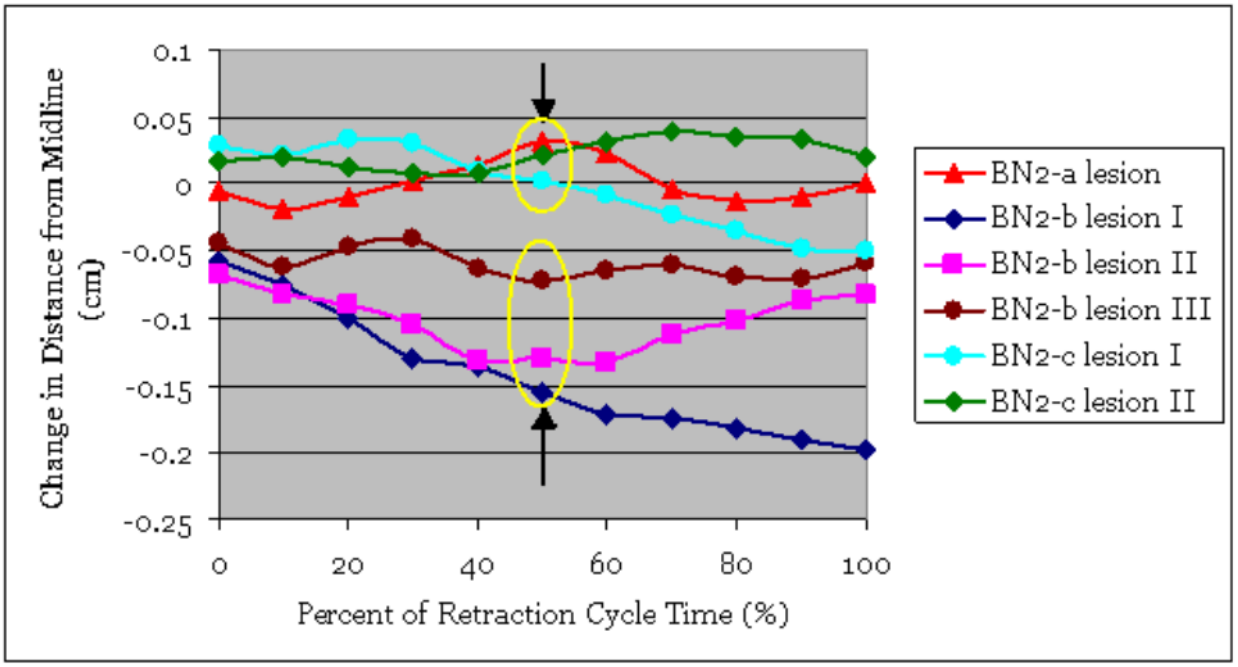


Figure 19. The difference in distance between pre-lesion and post-lesion behavior is plotted along the normalized time scale.

points at 10%, 20%, 30%, etc. of that particular observation. This is accomplished using a point-slope formula. Time at 0% represents when the radula halves close together immediately after peak protraction, and 100% represents when the jaw and/or radula are no longer clearly discernable after retraction.

In addition, observations show that the early phase of retraction (approximately 0% to 50% period) shows a clear deviation of BN2-b shift in comparison to BN2-a and BN2-c lesions. Measurement of the shift from the midline is more difficult due to jaw closure and possible realignment of the midline. In order to test the significance of the deviation at 50% of the retraction cycle time, a one-tailed t-test was performed for two variables of unequal variance. The resulting t-value was 0.01055, and therefore the difference between branch "b" lesions and lesion on the other branches is significant.

## DISCUSSION

Unilateral lesions on the branches of buccal nerve 2, responsible for innervation of the I1/I3/jaw complex, were performed to observe the effects on the protractive force during biting. The results support the hypothesis that unilateral lesions on branch "b" specifically would cause deficits in the peak protraction of biting. Furthermore, analysis reveals that unilateral lesions on branches "a" and "c" cause no significant alterations in normal biting behavior.

Normal biting behavior consists of a protraction phase, a peak protraction lasting for an extended period of time, and a retraction phase. Unilateral lesions allowed comparison between behaviors exhibited by each radula half. After BN2-b unilateral lesions, the radula began to retract significantly faster on the lesioned side. Observation of the differences in the distance from the radula center to the jaw plane midline between pre- and post-lesion behavior show that unilateral BN2-b lesions result in an increased retraction (i.e. greater shift of the radula center) towards the lesioned side. The results show that the early phase of retraction in particular clearly demonstrates this shifted behavior. During the late phase of retraction, measurement of the shift is slightly less reliable due to the closing of the jaws and possible re-centering of the jaw plane midline.

Unilateral lesions of BN2 on branches "a" and "c," however, do not show any significant difference in shift between pre- and post-surgery behavior, thus acting as controls surgery. The "b" branch has previously been shown to contract the posterior portion of I1/I3, whereas branches "a" and "c" contract the anterior portion. Thus, these results suggest that forces expressed by the posterior part of the I1/I3/jaw complex are necessary to sustain complete protraction near the peak of biting and slow retraction of the radula/odontophore. Thus, when this active ability is blocked, the impaired side will retract earlier and with a greater rate of change.

In addition to the observations presented in this study, sham lesions were also performed but have yet to be analyzed. Sham lesions follow the same method of anesthesia and surgical procedure as lesioned animals, but a neural lesion is not performed. Analysis of this data will strengthen our confidence in the results observed in control animals, as no neural lesion was imposed. Furthermore, additional statistical analysis, such as confidence intervals, would also aid in determining significant differences in behavior.

Error was one major consideration in the data analysis procedure, especially in the point configuration

in WinAnalyze. Though the software has an automatic tracking tool to follow a certain point, there is a large amount of deviation that must be corrected by hand. Future studies may include an additional means to measure deviation from the midline, such as comparing the heights of the radula halves or jaw width. Furthermore, future studies may measure the time from peak protraction to complete retraction in order to quantify the effects of a more rapid beginning of retraction (due to the lost protractive force).

These studies are helpful in further understanding the interactions between biomechanics and neural control not only in invertebrates such as *Aplysia*, but also other organisms in which muscle performs both force and skeletal support functions, i.e., tongues, trunks or tentacles. In particular, study of the neural control over context dependent muscles in *Aplysia californica* can provide insight into those of other organisms. As shown by previous studies, human muscle may also exhibit context dependent behavior. For example, elbow flexion deviation and postural variation can occur as a function of its context. The results of studies on invertebrates can be used towards understanding muscular function in humans and higher order animals. Furthermore, this understanding could be applied to the research and development of mechanical devices to replace muscles. For example, current research on prosthetics has focused on functional electrical stimulation (FES) to restore movement, sight, and other normal capabilities (Faghri *et al.* 1994 and Marsolais *et al.* 1987).

# REFERENCES


Buneo, C.A., Soechting, J.F., and Flanders, M. (1997) "Postural Dependence of Muscle Actions: Implications for Neural Control." The Journal of Neuroscience. 17(6): 2128-2142.

Chiel, H.J., Neustadter, D.M., Morton, D.W., Rundo, L., and Crago, P.E. "Context-Dependent Function of a Feeding Muscle in *Aplysia californica*." Unpublished observations.

Faghri, P.D., Rodger, M.M., Glaser, R.M., Bors, J.G., Ho, C., and Akuthota, P. (1994) "The effects of functional electrical stimulation on shoulder sublaxation, arm function recovery, and shoulder pain in hemiplegic stroke patients." Archives of Physical Medicine and Rehabilitation. 75(1): 73-79.

Lawrence, J.H. and Nichols, T.R. (1999a) "A three-dimensional biomechanical analysis of the cat ankle joint complex: I. Active and passive postural mechanics." Journal of Applied Biomechanics. 15(2): 95-105.

Lawrence, J.H. and Nichols, T.R. (1999b) "A three-dimensional biomechanical analysis of the cat ankle joint complex: II. Effects of ankle joint orientation on evoked isometric joint torque." Journal of Applied Biomechanics. 15(2): 106-119.

Mangan, E.V., Kingsley, D.A., Quinn, R.D., Sutton, G.P., Mansour, J.M., and Chiel, H.J. (2005) "A biologically inspired gripping device." Industrial Robot-an International Journal. 32(1): 49-54.

Marsolais, E.B., and Kobetic, R. (1987) "Functional electrical stimulation for walking in paraplegia." The Journal of Bone and Joint Surgery. 69(5): 728-733.

Murray, W.M., Delp, S.L., and Buchanan, T.S. (1998) "Variation of muscle moment arms with elbow and forearm position." Journal of Biomechanics. 28(5): 513-525.

Neustadter, D.M., Drushel, R.F., Crago, P.E., Adams, B.W., and Chiel, H.J. (2002a) "A kinematic model of swallowing in *Aplysia californica* based on radula/odontophore kinematics and *in vivo* magnetic resonance images." The Journal of Experimental Biology. 205: 3177-3206.

Neustadter, D.M., Drushel, R.F., and Chiel, H.J. (2002b) "Kinematics of the buccal mass during swallowing based on magnetic resonance imaging in intact, behaving *Aplysia californica*." The Journal of Experimental Biology. 205: 939-958.

Sutton, G.P., Mangan, E.V., Neustadter, D.M., Beer, R.D., Crago, P.E., Chiel, H.J. (2004) "Neural control exploits changing mechanical advantage and context dependence to generate different feeding responses in Aplysia." Biological Cybernetics. 91(5): 333-345.

Ye, H., Morton, D.W., and Chiel, H.J. (2006) "Neuromechanics of Coordination during Swallowing in *Aplysia californica*." The Journal of Neuroscience. 26(5): 1470-1485.